⌘ *Author's Choice*

THE JOURNAL OF BIOLOGICAL CHEMISTRY VOL. 284, NO. 5, pp. 3136–3147, January 30, 2009

Nuclear Factor Y Is Required for Basal Activation and Chromatin Accessibility of Fibroblast Growth Factor Receptor 2 Promoter in Osteoblast-like Cells*[S]

Received for publication, December 1, 2008 Published, JBC Papers in Press, December 1, 2008, DOI 10.1074/jbc.M808992200

Fenyong Sun[‡1], **Qiuling Xie**[‡1], **Ji Ma**[‡], **Songhai Yang**[§], **Qiongyu Chen**[‡], **and An Hong**[‡2]

From the [‡]*Institute of Genetic Engineering, Jinan University, National Engineering Research Center of Genetic Medicine, Key Lab for Genetic Medicine of Guangdong Province, Guangzhou 510632, China and* [§]*Shaoguan Tielu Hospital, Shaoguan, 512023, Guangdong, China*

Fibroblast growth factor receptor 2 (FGFR2) plays an important regulatory role in bone development. However, the regulatory mechanisms controlling FGFR2 expression remain poorly understood. Here we have identified a role for the nuclear factor Y (NF-Y) in constitutive activation of FGFR2. A unique DNase I hypersensitive site was detected in the region encompassing nucleotides −270 to +230 after scanning a large range covering 33.3 kilobases around the transcription start site of FGFR2. Using a PCR-based chromatin accessibility assay, an open chromatin conformation was detected around the proximal 5′ fragment of FGFR2 gene. Deletion constructs of the 5′-flanking region of FGFR2 were fused to a luciferase reporter gene. After transient transfection in C3H10T1/2, ME3T3-E1, and C2C12 as well as primary osteoblasts, a minimal region −86/+139 that is highly homologous to the human sequence and bears a CCAAT box was identified as the core promoter. Electrophoretic mobility shift assay supershift and chromatin immunoprecipitation demonstrated that the CCAAT box was the binding site for NF-Y. Deletion of NF-Y consensus sequence resulted in the total loss of NF-Y promoter activity. Overexpression of NF-Y protein and transfection of NF-Y small interfering RNAs in the cells substantially changed the promoter activity. Moreover, NF-Y small interfering RNAs greatly inhibited the endogenous FGFR2 transcription level and the chromatin accessibility and H3 acetylation across the promoter. Taken together, our results demonstrate that interaction of NF-Y at the CCAAT box is pivotal to FGFR2 gene transcription partly through the construction of a local open chromatin configuration across the promoter.

Fibroblast growth factor 2 (FGF2),[3] a member of the heparin binding growth factor family of mitogens, plays an important role in a range of normal physiological processes. Human and mouse genetic studies have established that FGF signaling also plays an essential role in skeletal development. FGF2 is produced by osteoblasts and stored in a bioactive form in the extracellular matrix (1, 2), where it acts as a local regulator of bone formation.

The FGF family of molecules transduces signals to the cytoplasm via a family of transmembrane receptors with tyrosine kinase activity(3, 4). Four distinct gene products encode highly homologous FGF receptors (FGFRs 1–4). FGFR2 is expressed in mesenchymal cells during condensation of mesenchyme before deposition of bone matrix at early stages of long bone development and is also expressed in the cranial suture. Later in development and in the postnatal life, FGFR2 is found in preosteoblasts and osteoblasts together with FGFR3. It was found that the recessive phenotype of FGFR2$^{-/-}$ mice is characterized initially by decreased expression of Cbfa1/Runx2 and retarded long bone ossification (5). Gain-of-function mutations in FGFR2 were found to induce changes in osteoblast proliferation, differentiation, and survival in mice and humans (6, 7). In human osteoblasts it was found that single missense point mutations (S252W and P253R) of FGFR2 activate the expression of early and late osteoblast differentiation genes, including alkaline phosphatase, type I collagen (COLIA1), and osteocalcin *in vitro* and *in vivo* (7, 8), a phenotype that is mediated in part through protein kinase C activation(9). These suggest that FGFR2 is a positive regulator of ossification.

NF-Y is a heterotrimeric transcriptional activator composed of three subunits (NF-YA, -B, and -C), which complexes with CCAAT box sequences (10). NF-Y subunit sequences are highly conserved among eukaryotes, and both NF-YB and NF-YC contain conserved putative histone fold motifs (11), showing most similarity to histones H2B and H2A. Thus, NF-Y subunits are capable of participating in formation of the histone octamer (12). Studies from several laboratories have suggested that NF-Y functionally and physically interacts with other transcription factors or nuclear proteins both *in vitro* and *in vivo* (13, 14). NF-YB and NF-YC have been demonstrated to interact with TATA-binding protein (TBP) *in vitro* (15), and NF-Y may, therefore, serve a structural role by recruiting TBP and/or

* The work was supported by 211 project, National Natural Science Foundation of China Grant 30400270, National 973 program Grant 2001CB510106, and Science and Technology program of Guangzhou Grant 2006Z1-E0031. The costs of publication of this article were defrayed in part by the payment of page charges. This article must therefore be hereby marked "*advertisement*" in accordance with 18 U.S.C. Section 1734 solely to indicate this fact.

⌘ *Author's Choice*—Final version full access.

[S] The on-line version of this article (available at http://www.jbc.org) contains supplemental Figs. 1 and 2.

[1] These authors contributed equally to this work.

[2] To whom correspondence should be addressed. Tel.: 86-020-85221983; Fax: 86-020-85221983; E-mail: tha@jnu.edu.cn.

[3] The abbreviations used are: FGF, fibroblast growth factor; FGFR2, FGF receptor 2; NF-Y, nuclear factor Y; EMSA, electrophoretic mobility shift assays; ChIP, chromatin immunoprecipitation; CHART-PCR, chromatin accessibility by real-time PCR; AR-S, alizarin red-S; BMP-2, bone morphogenetic protein 2; OB, osteoblasts; TBS, Tris-buffered saline; 5′-RLM-RACE, RNA ligase-mediated rapid amplification of 5′ cDNA ends; siRNA, small interfering RNA; kb, kilobases.

TAFIIs to connect upstream activators with the general polymerase II transcription machinery (16, 17). The interaction between NF-Y and GCN5 results in the modulation of NF-Y transactivation potential (18). Chromatin structure plays a vital role in transcriptional regulation by restricting the access of transcription-associated proteins to promoters, and it is likely that the interaction of NF-Y with histones and with other coregulators of transcription performs a critical and central function in the organization of core promoter activation.

Despite the extensive studies reviewed above, transcription factors that interact with the FGFR2 proximal promoter region have yet to be identified and functionally characterized. The aim of the present study was to define the functional cis-acting DNA elements responsible for basal activity of the FGFR2 core promoter in mouse osteoblast-like cell lines and thereby provide a basic model to aid future studies of FGFR2 promoter regulation. We find that one CCAAT box within the mouse FGFR2 proximal promoter region can specifically bind NF-Y transcription factors and that mutation or deletion of these sites diminishes FGFR2 promoter activity. Chromatin immunoprecipitation (ChIP) assays demonstrated the *in vivo* occupancy of the FGFR2 promoter by NF-Y transcription factor. We also showed that overexpression of NF-Y proteins results in the activation FGFR2 promoter, and knock down of NF-Y expression level leads to down-regulation of FGFR2 mRNA level and inhibition of FGFR2 transcriptional activity. Moreover, NF-Y is able to "open" and maintain the local chromatin structure across the FGFR2 promoter. We also demonstrated that NF-Y affected the effects of BMP-2 on FGFR2 expression and even the osteogenesis through controlling the basal expression of FGFR2.

EXPERIMENTAL PROCEDURES

Materials and Cell Culture—Antibodies against NF-YA, -B, and -C were purchased from Santa Cruz Biotechnology Inc. Antibody to diacetyl-H3 was obtained from Upstate Biotechnology Inc. Antibody against FLAG was purchased from Cell Signaling Technology. Calvaria from newborn mice were dissected free of surrounding muscles and soft tissues and washed in phosphate-buffered saline containing penicillin and streptomycin. Isolated calvaria were sequentially digested in α-minimum Eagle's medium containing 0.1% collagenase and 0.2% dispase at 37 °C. Digested fractions were collected every 10 min, and fractions 2–5 were pooled. Cells were collected by centrifugation and resuspended in α-minimum Eagle's medium supplemented with 10% fetal calf serum. C3H10T1/2, MC3T3-E1, and C2C12 cell lines were purchased from ATCC and maintained in Eagle's basal medium, α-minimum Eagle's medium. and Dulbecco's modified Eagle's medium (Invitrogen), respectively, with 10% fetal bovine serum, penicillin, and streptomycin.

RNA Ligase-mediated Rapid Amplification of 5′ cDNA Ends (5′-RLM-RACE)—The GeneRacer system (Invitrogen), based on RNA ligase-mediated and oligo-capping rapid amplification of cDNA, was carried out according to the manufacturer's instructions. The kit ensures the amplification of only full-length transcripts by eliminating truncated messages from the amplification process. FGFR2-specific primer located in the first exon (RACE-EX1, 5′-GGCGAGTAGTGAACACTCGCAGCGCTC-3′, + 230 to +204) was used for reverse transcription. The 5′ cDNA end was amplified by PCR using the GC-Rich PCR system (Takara).

Nuclei Isolation and DNase I Hypersensitivity Analysis—For nuclei isolation, cells were collected and resuspended in 3 ml of cold lysis buffer (0.35 M sucrose, 60 mM KCl, 15 mM NaCl, 2 mM EDTA, 0.5 mM EGTA, 15 mM Hepes, pH 7.4, 0.6% Nonidet P-40, 1 mM phenylmethylsulfonyl fluoride, 0.15 mM spermine, 0.5 mM spermidine) and incubated on ice for 5 min. The lysate was spun at 800 × *g* for 5 min at 4 °C. The nuclear pellet was washed twice in 2 ml of nuclei wash buffer (lysis buffer without Nonidet P-40) and spun at 800 × *g* for 5 min at 4 °C. The nuclei were resuspended in 500 μl of nuclei storage buffer consisting of 60 mM KCl, 15 mM NaCl, 0.1 mM EDTA, 0.1 mM EGTA, 75 mM Hepes, pH 7.5, glycerol (40% by volume), 0.1 mM phenylmethylsulfonyl fluoride, 0.15 mM spermidine, 0.5 mM dithiothreitol, and stored at −70 °C until needed. Nuclei were spun at 800 × *g* and resuspended in a nuclease digest buffer consisting of 10 mM Tris-HCl, pH 7.5, 10 mM NaCl, 5 mM $MgCl_2$, and 0.1 mM $CaCl_2$. The nuclei were digested with increasing concentrations of DNase I (Roche Applied Science) that ranged from 0 to 80 units per reaction for 10 min at 37 °C. The DNase I digestion was stopped by the addition of an equal volume of stop solution consisting of 20 mM Tris-HCl, pH 7.5, 10 mM EDTA, 0.6 M NaCl, 1% SDS, and 400 μg/ml proteinase K, and the digests were incubated at 55 °C for overnight. The genomic DNA was purified from each reaction by phenol/chloroform and subsequent ethanol precipitation. The precipitated DNA was resuspended in 10 mM Tris, pH 7.4, and quantitated by optical density. Approximately 20 μg of DNase I-treated DNA was digested with EcoRV and separated by size on a 0.8% agarose gel using 1× Tris-buffered EDTA buffer. The DNA was transferred to a nylon membrane, and Southern analysis was performed using a ^{32}P-labeled mouse FGFR2-specific DNA fragment as the probe. The DNase I hypersensitivity sites were visualized by exposing the blot to x-ray film for 24–36 h.

Chromatin Accessibility Analysis of Chromatin Structure—Accessibility of DNA to digestion with DNase I was analyzed using chromatin accessibility by real-time PCR (CHART- PCR) (29). Briefly, cell nuclei were resuspended in DNase I digestion buffer (10 mM Tris-HCl, pH 7.5, 10 mM NaCl, 5 mM $MgCl_2$, and 0.1 mM $CaCl_2$). Aliquots of nuclei (5×10^6) were incubated with 50 units of DNase I for 10 min at 25 °C, and reactions were terminated by the addition of stop buffer (10 mM Tris-HCl, pH 7.6, 10 mM EDTA, 0.5% SDS, and proteinase K at 100 μg/ml). DNA was extracted by phenol-chloroform extraction. Genomic DNA was then extracted using the QIAmp kit (Qiagen). About 50 μg of DNA from nuclease-digested or non-digested control cells was used in real-time PCR with the primer sets listed in Table 1. Percent protection was calculated as the amount of DNA recovered from the digested cells relative to the control cells.

Chromatin Immunoprecipitation Assays—ChIP assays were performed according to the manufacturer's instructions (Active Motif). Briefly, 2×10^6 cells were fixed with 1% formaldehyde, washed with cold phosphate-buffered saline, and lysed in buffer. Nuclei were sonicated to shear DNA, and the lysates were pelleted and precleared. The protein-DNA com-

TABLE 1

Primers used for PCR procedure in the experiments

Italic letters indicate tagged Kpn I and Xho I sites in the sense and anti-sense primer for cloning.

Primers	Sequence
CHART-PCR	
P1	Forward: 5′-GCGCTTCATCTGCCTGGTCTTGGTCAC-3′
	Reverse: 5′-CCAAAACGACTTGGTACCCTTAAAATG-3′
P2	Forward: 5′-GCGGAACGGGCGCACGGACGATCGAA-3′
	Reverse: 5′-GGCGAGTAGTGAACACTCGCAGCGCTC-3′
P3	Forward: 5′-TGTCTCTTTGCGGCTGCTAGGCTTCGG-3′
	Reverse: 5′-TCGCCTCTCCCGGCTCTCTCCCCT-3′
P4	Forward: 5′-ACTGTGCACCAAAGCTGGCTAGGAAC-3′
	Reverse: 5′-CCGAAGCCTAGCAGCCGCAAAGAGACA-3′
P5	Forward: 5′-TGCCTGAGGCATTGAACATGGATTTGC-3′
	Reverse: 5′-ACCTTATGCCATTTACACACACGATTC-3′
Luciferase constructs	
pGL3/01 (−758/+139)	Forward: 5′-*ggtacc*GGCTTTTGGCCTTTAAGAAGGCAGGAA-3′
pGL3/02 (−567/+139)	Forward: 5′-*ggtacc*TTTTCTTGTCAGAATCTGGTTCTGTTA-3′
pGL3/03 (−453/+139)	Forward: 5′-*ggtacc*CTATTGTTCAGAGGAACAAGACAACGC-3′
pGL3/04 (−347/+139)	Forward: 5′-*ggtacc*CTATTCTAAGGTGTCTGAAGTTGCACA-3′
pGL3/05 (−215/+139)	Forward: 5′-*ggtacc*CAACAGGGTTCCGAGAGGTCATCTGTG-3′
pGL3/06 (−86/+139)	Forward: 5′-*ggtacc*GCGAGGCGCTGATTGGCAGAGCGGGCG-3′
Common (+139)	Reverse: 5′-*ctcgag*GGCCAGGAACACACAGGCAGCCCCCG-3′
pGL3/05M (−215/−86)	Forward: 5′-*ggtacc*CAACAGGGTTCCGAGAGGTCATCTGTG-3′
	Reverse: 5′-*ctcgag*GCTGGGGCAGTCCCGAGCCCCGCGCTG-3′
RT-PCR	
NF-YA	Forward: 5′-ccgagtttcctaaccacagg-3′
	Reverse: 5′-tgtcctgagaaagggcagag-3′
NF-YB	Forward: 5′-accagctggcttaataactgc-3′
	Reverse: 5′-gcctctgcttcagactccat-3′
18 S RNA	Forward: 5′-cctggataccgcagctagga-3′
	Reverse: 5′-tctagcggcgcaatacgaatg-3′
FGFR2	Forward: 5′-tcacaaccaatgaggaatac-3′
	Reverse: 5′-cagacagggttcataaggca-3′

plexes were incubated with protein A beads, the protein-DNA complexes were eluted in 1% SDS, 0.1 M $NaHCO_3$, and cross-links were reversed at 65 °C. DNA was recovered by phenol-chloroform extraction and ethanol precipitation then subjected to semiquantitative PCR analysis. Primers used in semiquantitative real time PCR were the same as used in CHART-PCR.

Electrophoretic Mobility Shift Assays (EMSAs)—EMSAs were performed using the EMSA kit (Promega). 5.0 μg of nuclear extract proteins were incubated in 15 μl of reaction containing 4% glycerol, 1 mM $MgCl_2$, 0.5 mM dithiothreitol, 0.5 mM EDTA, 50 mM NaCl, 10 mM Tris-HCl, pH 7.5, and 2.0 μg poly(dI-dC) with or without molar excess of unlabeled DNA competitors on ice for 15 min followed by the addition of the radiolabeled probe. For supershift assays, antibodies against NF-YA, NF-YB, or NF-YC were added to the reaction mixture 25 min before the addition of the probe. All DNA-protein complexes were resolved by electrophoresis on 5% native polyacrylamide. The following double-stranded oligonucleotides were used in EMSAs as probes and/or competitors: wild-type −80/−68 probe: 5′-GCGAGGCGCTGATTGGCAGAGCGGGC-3′; mutant −80/−68 probe: 5′-GCGAGGCGCTGGATCACAGAGCGGGC-3′.

Western Blot Analysis—Cells were harvested and lysed in 0.5 ml of lysis buffer (10 mM Tris-HCl, pH 7.6, 5 mM EDTA, 50 mM NaCl, 30 mM sodium pyrophosphate, 50 mM NaF, 0.1 mM Na_3VO_4, 1% Triton X-100, 1 mM phenylmethylsulfonyl fluoride and protease inhibitor mixture tablet (Roche Applied Science)). Lysates were clarified by centrifugation at 15,000 × *g* for 10 min. 30 μg of protein was processed for SDS-PAGE, which was performed on 12% gels. The proteins were electrophoretically transferred to Immobilon P (Millipore). The blots were blocked with 5% nonfat milk in Tris-buffered saline (TBS, pH 7.4) for 1 h and then incubated with antibodies in 5% nonfat milk in TBS. They were then washed with TBS and incubated with secondary antibodies conjugated with horseradish peroxidase in 5% nonfat milk in TBS. After washing with TBS, the bound antibodies were visualized by enhanced chemiluminescence (Pierce) and recorded on x-ray films.

Reverse Transcription-PCR—Total RNA was extracted and purified using the RNeasy Kit (Qiagen). The concentration of extracted RNA from each group was adjusted to 200 ng/μl based on the absorbance value measured at 260 nm. A 25-μl reaction mixture containing 2 μg of total RNA was reverse-transcribed to cDNA using SuperScript II RT polymerase (Invitrogen).

Semiquantitative PCR—PCR reaction mix was prepared using SYBR Green PCR Master Mix (Applied Biosystems). PCR conditions were as follows: 95 °C for 5 min, 45 cycles of denaturation at 95 °C for 15 s, annealing at 60 °C for 5 s, and extension at 72 °C for 30 s. PCR was carried out using the 7300 Real Time PCR System (Applied Biosystems). Fluorescence of each sample was determined after every cycle. Denaturation curves of PCR products were determined by increasing temperature at the rate of 0.1/min from 55 to 95. Fluorescence of samples was continuously traced during this period. All the melting curves of PCR products gave a single peak. Agarose gel electrophoresis of representative reactions was used to confirm amplification of unique fragments of predicted lengths. All the results are expressed as the means ± S.D. of three independent experiments. Relative gene expression levels were calculated as ratios of the mRNA levels normalized against those of 18 S rRNA.

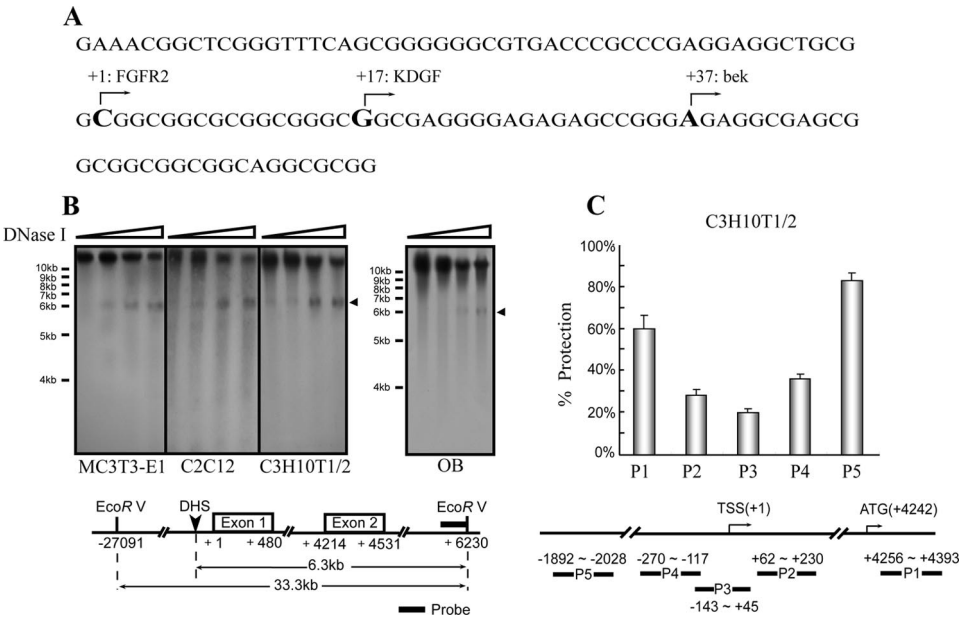

FIGURE 1. **Analysis of the FGFR2 promoter.** *A*, mapping the transcription start site of FGFR2 in C3H10T1/2. The experimentally determined transcription initiation site of the mouse FGFR2 promoter by 5′-RLM-RACE is denoted as +1. The cDNA sequences of KGFR and bek begin at position +17 and +37, respectively. *B*, DNase I hypersensitive site analysis of the FGFR2 promoter region. *Top panel*, nuclei from C3H10T1/2, C2C12, MC3T3, and primary osteoblasts were treated with increasing amounts of DNase I (*left* to *right*, shown by *triangles*). After DNA extraction and digestion with EcoR, they were hybridized with the probe shown in V. *Bottom panel*, the *arrowhead* shows bands (about 6.3 kb) due to DNase I cleavage. *C*, DNase accessibility of FGFR2 gene in C3H10T1/2 cells. *Top panel*, nuclei from C3H10T1/2 were harvested and treated with 50 units of DNase for 10 min at 25 °C. Then the genomic DNA was purified and quantitated relative to DNA I from undigested nuclei using the primers described in the *bottom panel* by quantitative PCR and listed as percent protected. Each *bar* represents the means ± S.D. of three independent experiments.

Transfection and Luciferase Assay—For transient transfections, plasmid DNA was transfected into cells using the Lipofectamine 2000 (Invitrogen). The plasmid phRL-TK vector (Promega) was always cotransfected as an internal control for transfection efficiency. After further cultivation for 24 h, the transfected cells were harvested, lysed, centrifuged to pellet the debris, and subjected to the luciferase assay. Luciferase activity was measured as chemiluminescence in a luminometer (PerkinElmer Life Sciences) using the Dual-Luciferase Reporter Assay System (Promega) according to the manufacturer's protocol. The results were expressed as the means ± S.D. of three independent experiments. Specific NF-YA small interfering RNA (siRNA) (5′-GAAGUGUUGAGGACAUUCAdTdT-3′), NF-YB (5′-GACUAAUUGAGGUGUUAAUdTdT-3′), or control scramble siRNA with no known homology to any mammalian genes (5′-GCGCGCUUUGUAGGAUUCGdTdT-3′) (20 nM) was transfected into cells using Lipofectamine 2000 according to the manufacturer's instructions.

Construction of Reporter Plasmids and Mutation—PCR procedures were used to generate 5′ stepwise deletion constructs of the FGFR2 promoter. PCR was performed using sets of oligonucleotide primers specific for the mouse FGFR2 gene sequence, of which the forward primer was KpnI-site-linked, and the reverse primer was XhoI-site-linked (Table 1). C3H10T1/2 genomic DNA was used to generate the pGL3/01 (−758/+139) construct, which was used as the template for the other constructs. These PCR products were digested with KpnI and Xho and subcloned into the KpnII/XhoI sites of the pGL3 Basic vector (Promega). Substitution mutation constructs were generated by the PCR-based site-directed mutagenesis kit (Takara) using the pGL3/06 plasmid as template. For eight-base substitutions, we introduced the nonspecific sequence ATGCATGC into the substitution sites and ATGCAT for 6-base substitutions. For pGL3/07 (−48/+109), pGL3/08 (+2/+139), and pGL3/09 (+102/+139), Erase-a-base kit (Promega) was used to generate the mutant constructs. The expression plasmids used were pCMV-NF-YA, pCMV-NF-YB, and pCMV-NF-YC, purchased from Invitrogen. All plasmids are under the control of the cytomegalovirus promoter.

Matrix Mineralization—After the cells became confluent, the medium was supplied with the mineralization medium containing 10% fetal bovine serum, 200 ng/ml BMP-2 (R&D), 10 mM β-glycerophosphate. The medium was changed every 3 days. The mineralized matrix was stained by alizarin red-S (AR-S). Briefly, at each time point the cells were washed twice with phosphate-buffered saline and fixed with 70% ethanol for 60 min. The fixed cells were incubated with 40 mM AR-S for 10 min with shaking. To minimize any nonspecific staining, the cells were rinsed 5 times with deionized water and once with phosphate-buffered saline for 20 min. The AR-S staining of the mineralization of the extra cellular matrix was photographed.

Statistical Analysis—Statistical evaluations were conducted using *t* test. *p* values less than 0.05 were considered to be statistically significant.

RESULTS

Identification of Transcription Initiation Site—To define the promoter region, we first identified the transcription start site of FGFR2 through 5′-RLM-RACE. Compared with the other often used methods, such as primer extension, nuclease protection assays, and classic 5′-RACE, 5′-RLM-RACE is more sensitive, and cDNA can be amplified only from full-length capped mRNA. In our study, total RNA from C3H10T1/2 cells was extracted for mapping the transcription start site. Using the GC-Rich PCR system and nested primers, the PCR products were cloned and sequenced. As shown in Fig. 1*A*, the transcription start site of FGFR2 in C3H10T1/2 cells is 17 nucleotides upstream from the beginning of the keratin growth factor receptor cDNA (19) or 37 nucleotides upstream from the reported bek cDNA (20).

Open Chromatin Structure around the Transcription Start Site—It is generally accepted that local chromatin structure affects gene transcription. We used the DNase I hypersensitivity site to reveal regions of open chromatin around the FGFR2

gene into three osteoblast-like cell lines, including C3H10T1/2 (a mouse embryonic fibroblast cell line), MC3T3-E1 (an osteoblast cell line), C2C12 (a myoblast cell line), and primary mouse osteoblasts (OB), all of which express the endogenous FGFR2 gene and may be induced to differentiate into mature osteoblasts. The genomic fragments between −27091 bp and +6230 bp (relative to the transcription start site) were analyzed. The results showed the appearance of two bands by Southern blot. The band of 33.3 kb represents the original EcoRV-EcoRV restriction fragment of FGFR2, and the lower band represents a single DNase I hypersensitive site that was estimated to be about 6.3 kb upstream of the EcoRV site at +6230 bp, adjacent to the transcription start site of FGFR2 promoter, located at the −270/+230 (Fig. 1*B*). This result suggests that this DNase I hypersensitive site is associated with the basal transcription of FGFR2 in osteoblast-like cells.

To confine the DNase I hypersensitive site to more narrow regions, a recently described CHART-PCR assay was performed to further locate the DNase I hypersensitive site between nucleotides −270 and +230, which is about 6.5 and 6.0 kb from the probe used in DNase I hypersensitivity assays. CHART-PCR evaluates the accessibility of genomic DNA to nuclease (such as DNase I, restriction enzyme, or micrococcal nuclease) by comparing the quantity of intact DNA from a nuclease-treated sample to that of an untreated sample (21–27). Chromatin recovered from both DNase I-treated and untreated cells was quantitated by real-time PCR. In addition to the region between nucleotides −270 and +230, another two representative regions were also included in CHART-PCR analysis: nucleotides −1892 to −2028 is a distal region upstream the transcription start site and nucleotides +4256 to +4393 is a fragment in the open reading frame. Thus, we were able to evaluate the nuclease accessibility of FGFR2 gene from 5′ distal region to the open reading frame (Fig. 1*C*).

Nuclease accessibility is expressed as the percent protection level that is calculated as the amount of DNA recovered from the digested cells relative to the undigested cells and inversely proportional to the protection level. As shown in Fig. 1*C*, DNase I digested all regions of the gene in C3H10T1/2, with the protection levels ranging from 20% to 83% compared with undigested samples. The region spanning the proximal promoter (covered by primer sets P2, P3, and P4) was more sensitive to DNase I digestion (Fig. 1*C*); particularly, the P3-covered region (−143 to +45) exhibited the lowest protection level of about 20%. In comparison, higher levels of protection against DNase I digestion were seen at the +4256 to +4393 region and the −1892 to −2028 region (Fig. 1*C*). Thus, DNase I accessibility is limited to the proximal promoter region (especially to the region of −143 to +45) and correlates closely with the results of DNase I hypersensitivity assays.

Deletion Analysis of the FGFR2 Promoter—To examine the transcriptional activity of the sequences at the 5′ end of the FGFR2 gene, various fragments of the proximal sequence were cloned upstream of the firefly luciferase reporter gene. A 5′ deletion series with a fixed 3′ end at the +139 position (relative to transcription start site) we generated through PCR amplification from genomic DNA of C3H10T1/2 cells. The constructs were transfected into C3H10T1/2, MC3T3-E1, C2C12, and primary OB. Although there were probably repressing activities between nucleotides −86 and −215, all the deletion constructs (containing −86/+139 fragment) tested were capable of inducing a significant increase in luciferase activity compared with that of a promoter-less vector (pGL3-Basic) (Fig. 2). This observation suggests that the most proximal 225 nucleotide of the FGFR2 gene is capable of initiating transcription. To confirm the role of the sequence between −86 and +139 (the proposed core promoter), a 3′ terminal deletion without this sequence was tested for promoter function in the cell lines. The results showed that when the proximal sequences are deleted, promoter activity was reduced to background levels (Fig. 1). Identical results were obtained with all the cell lines. These results demonstrate that the sequences between −86 and +139 are necessary for transcriptional initiation.

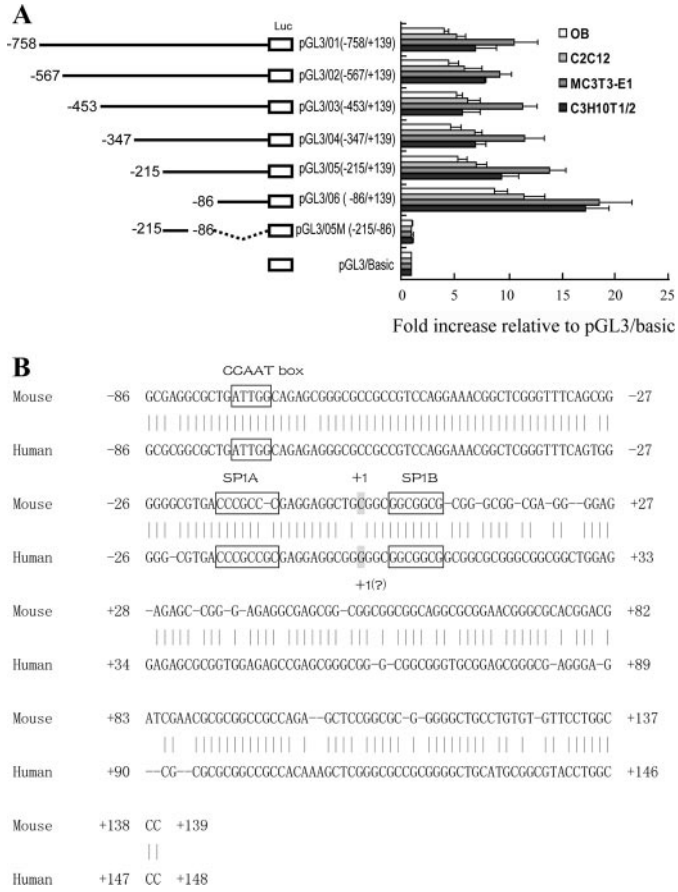

FIGURE 2. **Functional analysis of mouse FGFR2 promoter in C3H10T1/2, MC3T3-E1, C2C12, and primary OB.** *A*, a panel of 5′ terminal deletion-luciferase reporter constructs were transfected into the cell lines. Various constructs (1 μg) of the 5′-flanking region fused to the firefly luciferase reporter gene vector were co-transfected along with Renilla luciferase expression vector (0.2 μg) into cells. Firefly luciferase activity was normalized to Renilla luciferase activity, and the relative luciferase activities are presented as -fold increase over the promoterless pGL3 basic vector. Each *bar* represents the means ± S.D. of three independent experiments. *B*, comparison of mouse proximal promoter (−86 to +139) with human FGFR2 promoter sequences. The alignment of mouse and human FGFR2 promoter sequences was generated using the BLAST program. The experimentally determined transcription initiation site of the mouse FGFR2 promoter by 5′-RACE is denoted as +1. The transcription initiation site of the human promoter was not determined experimentally but set at the same position as in the mouse sequence based on strong sequence similarities. Transcription factor binding sites present in both sequences as identified by MatInspector are highlighted by *open boxes*.

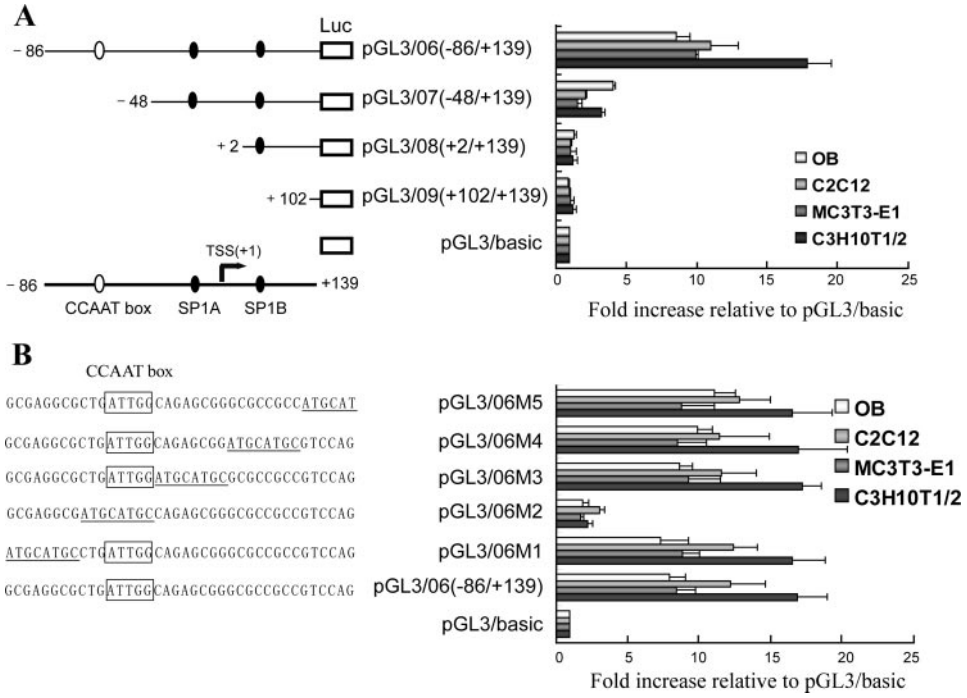

FIGURE 3. **Mutational analysis of the mouse FGFR2 core promoter (−86/+139).** *A*, the schematic structures of the reporter constructs are shown on the *left*. The length of each 5′-flanking segment, which is relative to the transcription start site, is indicated to the *left* of each line. Regulatory sequences (SP1 binding sites are indicated with *closed circles*, and the CCAAT box is indicated with *open circles*) are shown at the *bottom*. *Horizontal column lengths* on the *right* represent the means ± S.D. of three independent luciferase reporter assay experiments. *B*, scanning mutational analysis of the fragment −86/−48. As shown on the *left*, a series of 8-bp substitutions were made within the fragment −86/−48 of the reporter construct pGL3/06 (−86/+139). *Open boxes* represent the CCAAT boxes, and mutational bases are indicated with *underlined letters*. As shown on the *right*, *horizontal column lengths* represent the means ± S.D. of three independent luciferase reporter assay experiments.

To define potential cis-acting regulatory elements, we undertook a comparative analysis of the −86/+139 region between mouse and human genes. Alignment of the mouse fragment with the corresponding fragment from the human FGFR2 gene revealed striking similarities (82%). No apparent TATA box could be identified upstream of the transcription initiation site, but both promoters are highly GC-rich (mouse, 72%; human, 75%). A search for transcription factor binding sites using an online software (MatInspector) revealed two putative Sp1/Sp3 and one NF-Y potential binding sites that are similar in relative position and sequence in both species (Fig. 2).

A new series of deletion clones was then generated that allowed for the further characterization of FGFR2 promoter region from nucleotide −86 to +139. Because this DNA fragment is highly GC-rich and difficult for PCR reaction, we used Erase-a-base technique (Promega) instead of PCR amplification to produce three new deletion clones, denominated pGL3/07, pGL3/08, and pGL3/09. Deletion of nucleotides −86 to −48 (containing the NF-Y binding site) reduced luciferase activity to about 20%. Further deletions to nucleotide +2 (a fragment containing the SP1A binding site) inhibited the reporter activity further. Fragment +2 to +139 (containing the other SP1B binding site) and (+102/+139) lost all of the transcription activity (Fig. 3). These results suggest that binding of NF-Y transcription factors to FGFR2 proximal promoter may be responsible for most of the transcriptional activity of the promoter. To further test the possible NF-Y binding, we have generated a series of 8-base pair mutations between nucleotides −86 and −48 within pGL3/06 (−86/+139) construct through a PCR-based site-directed mutagenesis technique (Fig. 3*B*). Particularly, the mutation in pLUC3/06M2 which disrupts the NF-Y binding site reduced promoter activity by more than 90%. No significant changes in promoter activity had been observed in other mutant constructs (Fig. 3*B*).

Characterization of NF-Y Transcription Factors Binding to the FGFR2 Promoter Region in Vitro—To test DNA-protein interactions in the promoter region, we performed EMSA using the DNA sequence from −86 to −60 bearing the CCAAT box. One strong DNA-protein complex (BS1) and a weak fast-migrating complex (BS2) were detected (Fig. 4*A*). To determine whether the putative NF-Y binding site is involved in the formation of these complexes, a 10-, 50-, and 100-fold excess of unlabeled oligonucleotide corresponding to −86 to −60 sequence was used to compete with the complexes. As shown in Fig. 4*A*, the competitor competed away the complexes possibly by sequestering the available transcription factors present in the nuclear extract. These data indicate that the CCAAT box have protein binding capacity. In contrast, the unlabeled mutated oligonucleotide bearing the disrupted CCAAT box was unable to compete for protein binding capacity (Fig. 4*B*).

To test if NF-YA, NF-YB, and NF-YC are involved in the formation of the protein-DNA complexes detected in the EMSA, we performed supershift assays by using the polyclonal rabbit anti-NF-YA, -NF-YB, and -NF-YC antibodies. As illustrated in Fig. 4*C*, both the major complex BS1 and BS2 were inhibited by all the three antibodies in nuclear extracts from C3H10T1/2, MC3T3-E1, C2C12, and primary OB. Particularly, treatment of NF-YB antibody almost completely disrupted the major DNA-protein complex band. Preimmune rabbit IgG did not cause a shift or loss of the complexes, demonstrating the specificity of the super-shift assays. These results suggest that NF-Y can specifically interact with the wild-type −86 to −60 sequence probe.

Association of NF-Y with the FGFR2 Promoter in Vivo—We performed chromatin immunoprecipitation assay to examine whether NF-Y interacts with the FGFR2 promoter *in vivo*. As shown in Fig. 5, both anti-NF-YA and anti-NF-YB antibodies specifically enriched the region containing the FGFR2 proximal promoter. To confirm the specificity of the DNA binding activity of the factors at the FGFR2 promoter, PCR amplifications of the FGFR2 coding sequence, which has no binding sites for any

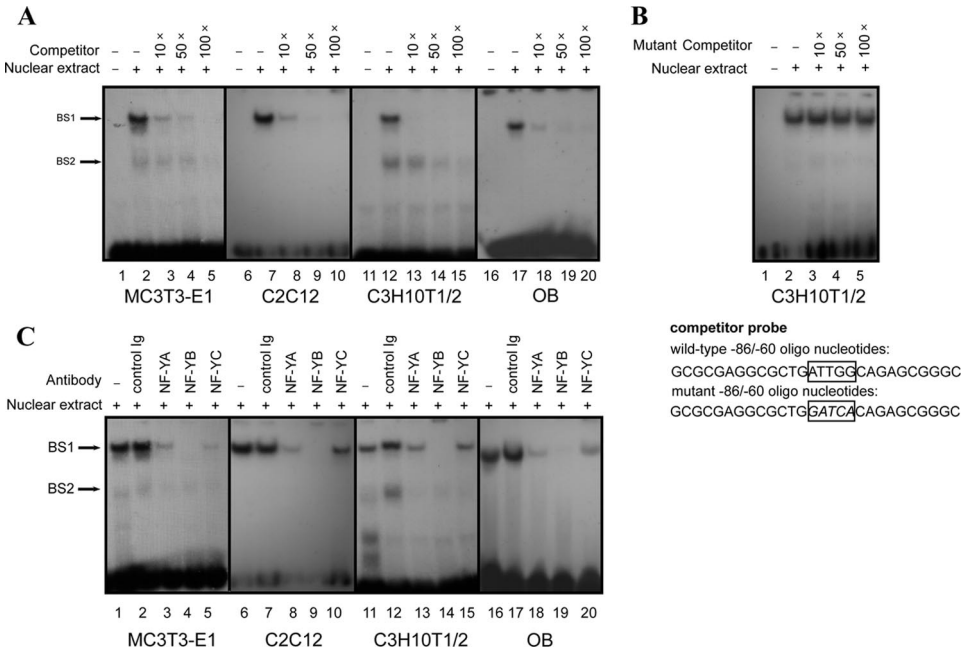

FIGURE 4. **Binding of NF-Y transcription factor to FGFR2 core promoter bearing the CCAAT box.** *A*, upon interaction with the nuclear extract of MC3T3-E1, C2C12, C3H10T1/2, and primary OB, −86/−60 probe generated two specific bands which was self-competed by increasing concentration of the cold oligo. *B*, no competition was observed when using the same amounts of −86/−60 CCAAT mutant oligo. *C*, interaction with anti-NF-YA, NF-YB, and NF-YC polyclonal antibodies resulted into a decrease in the shift band formation.

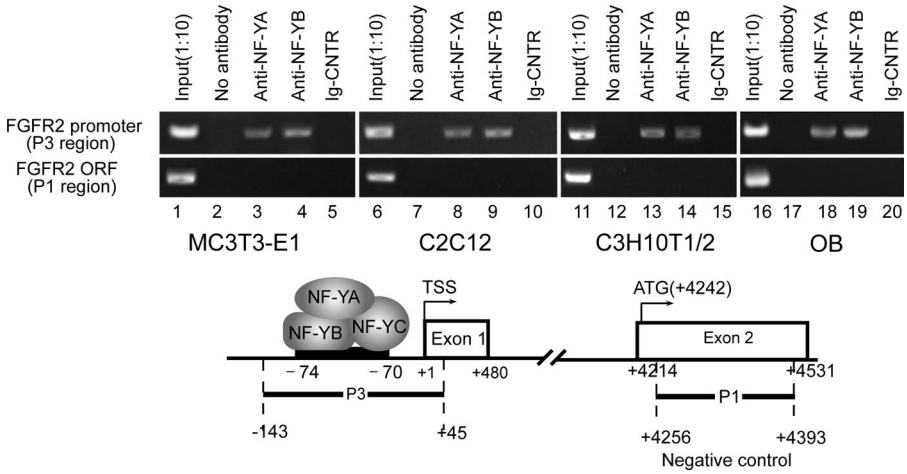

FIGURE 5. **Chromatin immunoprecipitation analysis.** Chromatin immunoprecipitation analysis was performed to confirm the interaction of NF-Y with the FGFR2 promoter *in vivo* in MC3T3-E1, C2C12, C3H10T1/2, and primary OB. PCR products from the ChIP assay were run on an agarose gel. As the negative controls (*CNTR*), the protein-DNA complexes were incubated without antibodies or with nonspecific IgG. The input DNA represents 1/10th of the starting material. Primers for an unrelated part of the FGFR2 open reading frame (*ORF*) were utilized for control reactions of the ChIP analysis. The relative positions of the primers are indicated in the *lower part* of the *figure*.

of the regulators tested, were included in parallel experiments as negative controls. The results of ChIP experiments performed with these antibodies indicate that the basal transcription of FGFR2 in living cells involves recruitment of NF-Y to its promoter. Taken together, the data further support that NF-Y is involved in the organization of the FGFR2 basal transcriptional apparatus.

NF-Y Is Sufficient and Necessary for Activation of FGFR2 Promoter—Overexpression studies were performed to further test the role of NF-Y in regulating FGFR2 promoter activation. Cells were transiently co-transfected with either pGL3/06 (bearing wild-type CCAAT box) or pGL3/06M2 (bearing mutant CCAAT box) and 1.0 μg NF-YA, NF-YB, and NF-YC expression vectors. As shown in Fig. 6*A*, transient expression of NF-YA alone or with NF-YB were able to stimulate the promoter activities, but co-expression of all three subunits together dramatically induced the activity of promoter constructs to a higher level. In contrast, the transcriptional activity from pGL3/06M2 after NF-Y overexpression was completely abolished. These results suggest that NF-Y transcription factors are sufficient to activate the FGFR2 promoter through interaction with the CCAAT box.

We next investigated the necessity of NF-Y in basal FGFR2 transcription. To address this, we inhibited NF-YA and NF-YB expression using siRNA. C3H10T1/2 cells were transfected with NF-YA- or NF-YB-targeted siRNAs and a scramble siRNA as control. Both the siRNAs reduced the two target mRNAs levels remarkably (Fig. 6*B*) and resulted in inhibition of the basal FGFR2 transcription level to 21 and 35% in NF-YA siRNA-transfected cells and NF-YB siRNA-transfected cells, respectively (Fig. 6*C*). The similar results were obtained after siRNA treatment with C2C12 and MC3T3-E1 and primary OB (supplemental Fig. 1). We also co-transfected the luciferase reporter construct pGL3/06 (−89/+139), containing the core promoter of FGFR2, with NF-YA or NF-YB-targeted siRNAs into C3H10T1/2 cells. The results showed that the transcriptional activation level of the fragment −89/+139 were greatly inhibited by either the NF-YA siRNA or the NF-YB siRNA (Fig. 6*D*). These data suggest that NF-Y transcription factors are indispensable for FGFR2 promoter activation.

NF-Y Transcription Factors Contribute to DNase I Accessibility and Histone Acetylation—Chromatin remodeling is an essential step during transcriptional regulation and controls accessibility to DNA binding factors (28). It has been postulated that binding of NF-Y proteins to CCAAT box is instrumental in maintaining an open chromatin configuration of the target promoters (29). We determined whether NF-Y transcription factors are necessary for an accessible configuration at the FGFR2 promoter.

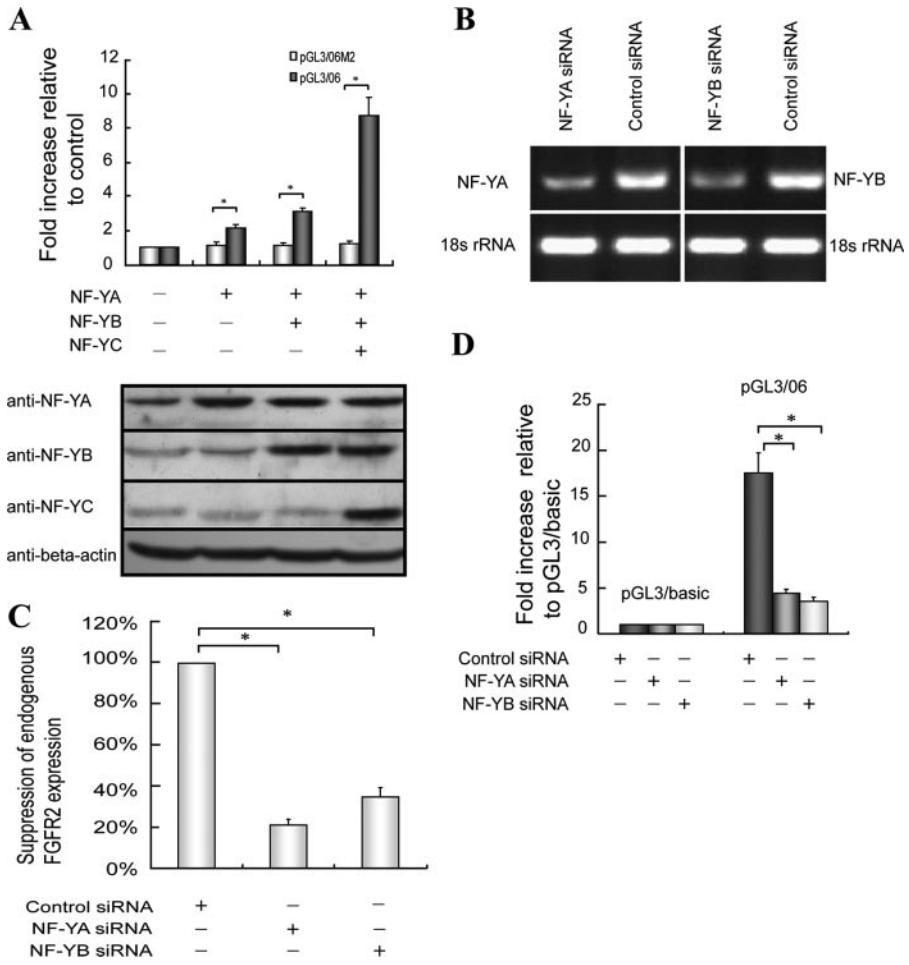

FIGURE 6. **Effects of NF-Y on FGFR2 core promoter activity.** *A*, overexpression of NF-Y promotes FGFR2 promoter activity. C3H10T1/2 cells were cotransfected with 1.0 μg of pGL3/06 (−89/+139) or pGL3/06M2 luciferase reporter constructs together with 1.0 μg of expression vectors encoding wild-type NF-YA, -B, and -C. After 48 h of culture cells were harvested, and the cell lysate was assayed for Renilla and luciferase assay. Data presented are the means of the three independent experiments performed in duplicate. The whole lysates were examined by immunoblotting with antibodies against NF-YA, -B, -C and β-actin. *B–D*, RNAi for NF-YA and NF-YB reduced FGFR2 transcription in C3H10T1/2 cells. C3H10T1/2 cells were transfected with NF-YA-targeted siRNA, NF-YB-targeted siRNA, or a control siRNA. Total RNA was collected after 48 h for assessment of transcription levels by RT-PCR. The PCR products of NF-YA, NF-YB, and 18 S rRNA were electrophoresed and stained with ethidium bromide. *B*, endogenous FGFR2 mRNAs were quantified by SYBR Green real-time PCR and normalized to 18 s rRNA. *C*, siRNAs were co-transfected with pGL3/06 or pGL3/basic into cells. Firefly luciferase activity was normalized to Renilla luciferase activity, and the relative luciferase activities are presented as -fold increase over the promoterless pGL3 basic vector. *D*, all the data were shown as means of three independent experiments ± S.D. *, $p < 0.01$, *versus* the controlled cells.

First, we investigate the possible roles of NF-Y proteins in regulating chromosome accessibility of FGFR2 promoter by CHART-PCR assays. NF-YA and NF-YB siRNAs were transfected into C3H10T1/2 cells, and cell nuclei were collected for DNase I digestion. Compared with control cells transfected with scramble siRNAs, knockdown of NF-YA or NF-YB expression remarkably promoted the protection level at the proximal promoter region (covered by P2, P3, and P4 primer sets as shown in Fig. 1C). In contrast, the −1892 to −2028 and +4256 to +4393 regions exhibited no significant changes in DNase I accessibility (Fig. 7*A*). These results indicate that NF-Y proteins are required for chromatin remodeling of FGFR2 gene.

The H3 subunits of the nucleosome octamer are capable of undergoing acetylation in a locus-specific manner, which reflects whether an area of the genome is actively transcribed. Moreover, hyperacetylation of histones is associated with increased physical accessibility of genes (30, 31). Because inhibition of NF-Y expression may result in a more closed chromatin configuration at the FGFR2 locus, we postulated that the histone acetylation level may also be decreased. ChIP assays were performed with the same primer sets as those used in CHART-PCR. Using antibodies specific for diacetylated H3 (K9 and K14) revealed a pattern of local acetylation at the proximal promoter region and 5′ region of the coding sequence. In both instances acetylation is more pronounced at the promoter region. On the other hand, DNA fragments at the distal region failed to be enriched in the precipitation, indicating that H3 acetylation of FGFR2 gene is localized to actively transcribed regions. Treatment of C3H10T1/2 cells with 20 nM NF-YA or NF-YB siRNA for 48 h reduced the H3 acetylation level remarkably at both the proximal promoter and 5′ coding sequence regions. At the −143 to +45 region, H3 acetylation was inhibited to 42 and 38% after NF-YA and NF-YB siRNAs treatment, respectively. Interestingly, knockdown of NF-Y proteins resulted in the inhibition of H3 acetylation by about 30% at the 5′ coding sequence region that is 4 kb downstream the CCAAT box, suggesting that NF-Y proteins may serve to control the histone modification in a long range across the FGFR2 gene.

Overexpression of FGFR2 Promotes BMP-2-induced Osteogenesis—BMPs are the only signaling molecules that can singly induce *de novo* bone formation at orthotopic and heterotopic sites. To provide evidence for the functional role of FGFR2 in BMP-2-induced osteogenesis, we introduced the gene constructs for the fusion proteins of FGFR2-FLAG into C3H10T1/2 cells. After stable transfection into C3H10T1/2, three clones (C1-C3) were selected as determined by Western blotting using the anti-FLAG antibody (Fig. 8*A*). In the mineralized nodule formation analysis visualized by AR-S staining, we found that overexpression of FGFR2 significantly promoted matrix mineralization in all the three clones compared with the control (Fig. 8*A*). Additionally, stable transfection of the dominant negative form of FGFR2 and dominant negative FGFR2-FLAG (clones dC1-dC3), which contains only the extracellular fragment of the protein and was secreted into culture medium as soluble FGFR2, slightly inhibited mineralization (Fig. 8*A*). These data suggest that activation of FGF sig-

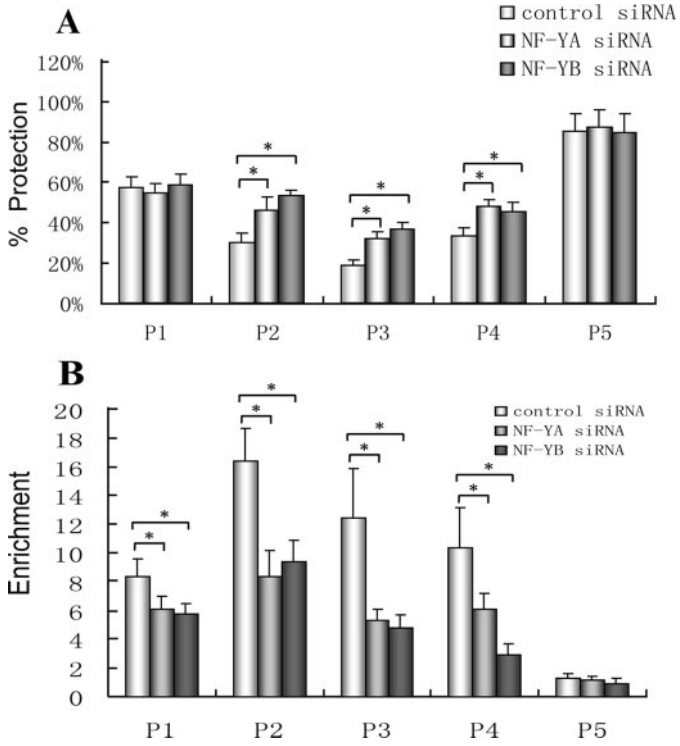

FIGURE 7. **RNAi for NF-YA and NF-YB reduces nuclear accessibility and H3 acetylation at FGFR2 gene.** C3H10T1/2 cells were transfected with 20 nm NF-YA, F-YB siRNA, or a control scramble siRNA. Nuclei were harvested after 48 h for further assessment. *A*, nuclei were treated with 50 units of DNase I for 10 min at 25 °C. Then the genomic DNA was purified and quantitated relative to DNA from undigested nuclei using the primers described in Fig. 1*C* and listed as percent protected. *B*, nuclei were precipitated with antibody specific for diacetylated H3 (K9 and K14). After DNA recovery the precipitates were evaluated by real-time PCR for the level of enrichment over the negative control with the primers shown in Fig. 1*C*. Each *bar* represents the means ± S.D. of three independent experiments. *, $p < 0.01$, *versus* the controlled cells.

nal pathway promotes BMP-2-stimulated osteogenesis in C3H10T1/2 cells.

The Effects of NF-Y on BMP-2-stimulated FGFR2 Expression—We further examined the expression level of FGFR2 in BMP-2-elicited osteogenesis by quantitative RT-PCR. As shown in Fig. 8, *B* and *C*, FGFR-2 expression was dose- and time-dependently up-regulated upon BMP-2 exposure. The similar results had been observed with C2C12, MC3T3-E1, and primary OB (supplemental Fig. 2). Unfortunately, we failed to identify the BMP-2-responsive element on FGFR2 promoter after searching a long range of 33.3 kb around the transcription start site by DNase I hypersensitivity assays using the probe as shown in Fig. 1*B* (data not shown). Then we hypothesized that the basal activation of FGFR2 promoter determined by NF-Y might be important for BMP-2-induced FGFR2 expression. As shown in Fig. 8*D*, inhibition of NF-YA and -B expression significantly suppressed both the basal and BMP-2-induced endogenous FGFR2 levels in C3H10T1/2 to the same extent. Taken together, although NF-Y does not mediate BMP-2-stimulated FGFR2 expression, it affects the BMP-2 effects on FGFR2 and even the osteogenesis (enhanced by FGF/FGFR2 signal pathway) through controlling the basal expression of FGFR2.

DISCUSSION

In this work we have analyzed the FGFR2 core promoter and found the specific interaction of NF-Y with the FGFR2 promoter through a CCAAT box located between nucleotide −74 and −70. To our knowledge, these data provide the first demonstration that the functional FGFR2 core promoter is composed of a CCAAT box. We show that in this core promoter (i) NF-Y binding at the CCAAT box is crucial for FGFR2 promoter activity, (ii) the two putative Sp1 boxes adjacent to the CCAAT box have no obvious activity, and (iii) NF-Y binding may result in an open chromatin configuration associated with local histone acetylation. Therefore, the present study delineates the fundamental elements of a core promoter structure that will be helpful for future studies on the differential regulation of FGFR2 expression in osteoblast.

NF-Y is an ubiquitous transcription factor that activates the basal transcriptional activity of various promoters through CCAAT boxes. More than 25% of eukaryotic promoters contain CCAAT boxes, in most cases within 100 bp from the transcription start sites (10). NF-Y may create a core promoter architecture that is suitable for assembly of a preinitiation complex. In a previous study, Duan *et al.* (32) have shown that a CCAAT box is required for the formation of the transcription initiation complex containing RNAP II, TATA-binding protein, and TFII B. In our study overexpression of NF-Y subunits could activate the FGFR2 promoter, and knockdown of NF-Y expression resulted in an inhibition of the promoter activation as well as endogenous FGFR2 transcription level. Therefore, we show directly that NF-Y is crucial for FGFR2 promoter activity in osteoblast-like cells.

The promoter of the FGFR2 gene resides in a CpG island that lacks the classical TATA box motifs found in many eukaryotic promoters. Sequence analysis of the FGFR2 promoter revealed two putative Sp1 binding sites (GC boxes) within a 50-bp DNA fragment, designated Sp1A and Sp1B. The positioning of the basal transcriptional machinery in a TATA-less promoter can occur independent of InR sequences when Sp1 binding sites are present (15, 17, 33–35). In such instances Sp1 is capable of stabilizing transcriptional initiation complexes downstream. In this report localization of the start site of transcription was achieved through 5′-RLM-RACE, and it was shown that transcriptional initiation occurs between the two putative Sp1 binding sites. Our start site is localized to the same position as that previously described by Skorecki and co-workers (36), strongly suggesting that the two Sp1 binding sites could facilitate organization of the transcription initiation complex. In fact, as revealed by luciferase reporter assays, pGL3/07 (containing both the Sp1 binding sites) gave to an average of 2-fold activation of luciferase activity in all the three cell lines compared with the control pGL3/basic vector. In contrast, pGL3/08 (containing only the Sp1B binding site) exhibited no significant difference in transcription activity compared with the control vector (Fig. 3). These results suggested that Sp1A may serve as another crucial transcriptional activator in addition to NF-Y. However, *in vitro* DNA binding studies (EMSA) using the −48 to +2 fragment as the labeled probe demonstrated no apparent DNA-protein complexes (data not shown). Anti-Sp1/Sp3 anti-

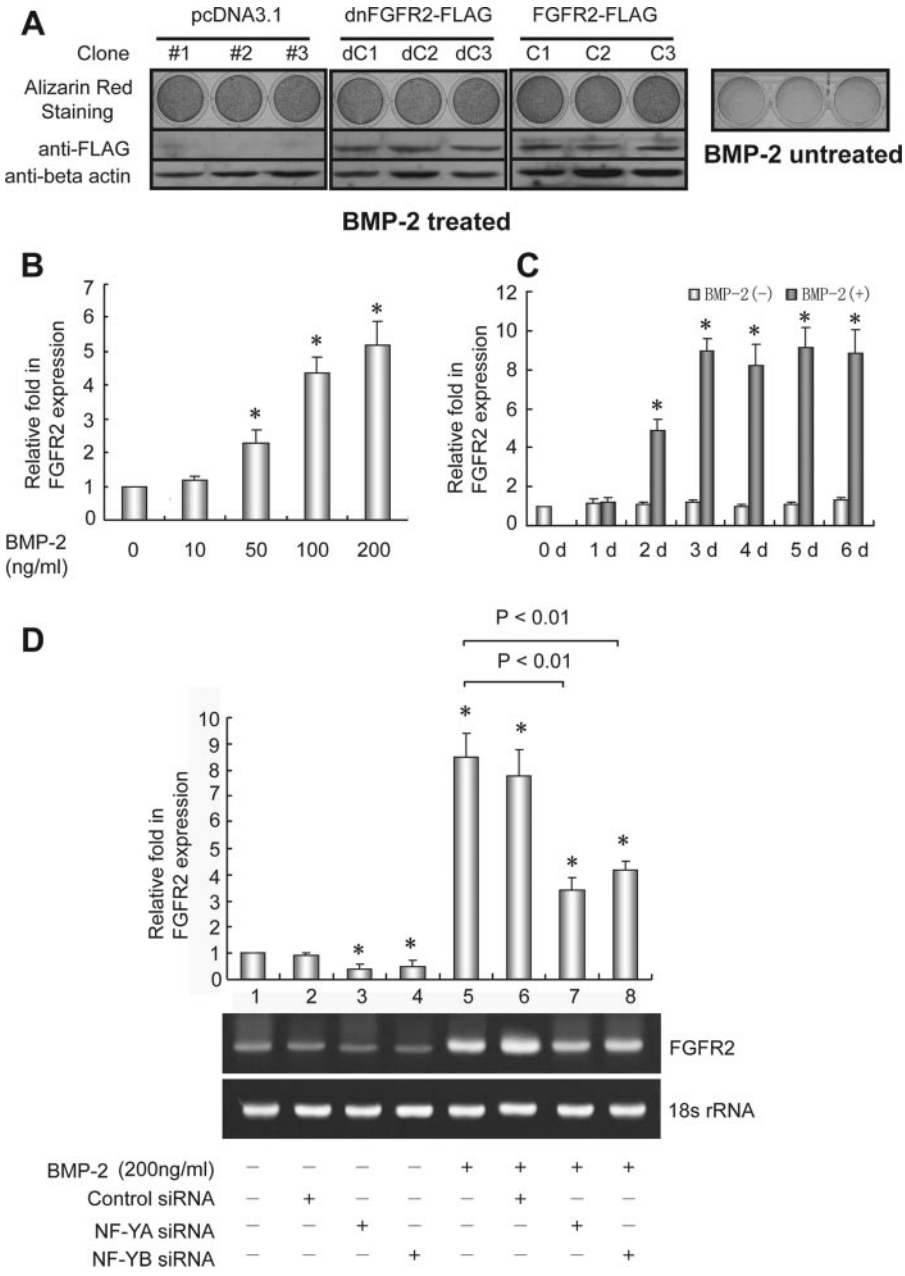

FIGURE 8. **NF-Y is important for BMP-2-induced FGFR2 expression.** *A*, FGFR2, dnFGFR2 (dominant negative form) expressing vectors and pcDNA3.1 were stably transfected into C3H10T1/2. Three clones of each transfection were isolated and subjected to Western blotting with anti-FLAG monoclonal antibody (*middle panel*). Upon BMP-2 (200 ng/ml) exposure for 2 weeks, the mineralization was evaluated by AR-S staining (*top panel*). *B* and *C*, C3H10T1/2 cells were incubated with the different dosages of BMP-2 for 3 day (*B*) or for the different time in the presence of 200 ng/ml BMP-2 (*C*), and total RNA was extracted for measurement of FGFR2 mRNA expression level by semiquantitative RT-PCR. *D*, C3H10T1/2 cells were transfected with NF-YA-targeted, NF-YB-targeted, or a control siRNA. Six hours after transfection the cells were treated with or without 200 ng/ml BMP-2. Total RNA was collected after 3 days for assessment of FGFR2 transcription levels by quantitative RT-PCR (*top panel*). The PCR products were electrophoresed and stained with ethidium bromide for visualization (*bottom panel*). *, $p < 0.01$ *versus* the controlled cells. All data were shown as means of three independent experiments ± S.D.

bodies also failed to enrich the DNA fragment in the precipitates as demonstrated by ChIP assays (data not shown). Because Sp1 and NF-Y have been shown to coordinately regulate many gene promoters and to physically interact with each other and with TATA-binding protein as well as general transcription factors (17, 37, 38), we cannot rule out the possibility that coordination of the factors binding to Sp1 sites and the CCAAT box constitute the FGFR2 core transcription machinery. Therefore, we created the combinational mutation constructs in which double or multiple site-directed mutation of the CCAAT box, Sp1A, and Sp1B binding sites were introduced into the reporter vector. But the data revealed no significant coordination among the three binding sites (data not shown). However, we cannot rule out that the contribution of Sp1A and Sp1B may vary in different cellular contexts. Finally, it should be noted that other binding sites for transcription factors not yet identified may regulate FGFR2 promoter function through the −48/+2 (Fig. 6) promoter fragment. A detailed mutation scanning analysis will be needed to identify such sites.

We also examined the role of NF-Y in regulating the chromatin structure of FGFR2 promoter. It is generally accepted that chromatin structure serves as an important means to control gene expression. An open chromatin configuration, which is more accessible to transcription factors and general transcription apparatus, is necessary for substantial activation of gene transcription. Here, we present the first evidence that binding by NF-Y may produce a more open chromatin structure across FGFR2 promoter.

Biochemical analyses of the NF-Y complex have demonstrated that the NF-YB:YC subunits associate through a subdomain in the DNA binding subunit interaction domain (39), referred to as the histone-fold "handshake" motif (11, 40), which resembles an α-helical structure first identified in the core histone proteins as primarily responsible for dimerization of the H2A/H2B and H3/H4 histone pairs. The NF-YB:YC histone-fold is most related to histones H2B/H2A (40) and similarly contains a number of hydrophobic amino acids that project along one face of an α-helix. Thus, NF-Y has a high intrinsic affinity for nucleosomal structures thanks to the NF-YB-NF-YC histone-like subunits (12, 41) and thereby disrupts the compaction of the chromatin, resulting in a more open configuration. In our study we observed that knockdown of NF-Y expression may drastically inhibit the accessibility to DNase I and as a result suppresses the endogenous FGFR2 transcription level. These findings strongly

support the hypothesis that binding of NF-Y presets the local chromatin configuration for FGFR2 promoter activation.

In a previous study NF-Y has been shown to interact with the coactivator p300 and P/CAF (p300/CBP-associated factor), which possesses a histone acetyltransferase activity important for transcriptional activation (18, 42). It is well known that hyperacetylated H3 or H4 may promote the release of DNA from the core histones, reduce nucleosome occupancy, and thus, increase chromatin accessibility to transcription apparatus. In fact, we did observe H3 hyperacetylation at the proximal FGFR2 promoter, propagating downstream even into the open reading frame (covered by P1 primers, shown in Fig. 7*B*). Importantly, suppression of NF-Y transcription by siRNAs reduces the acetylation level throughout all the aforementioned acetylated regions including the 5′ open reading frame region.

In this study we investigated the role of FGFR2 on osteoblast differentiation by characterizing the phenotype of C3H10T1/2 cells transfected with the full-length mouse FGFR2 gene and the dominant negative form. We provide the first evidence that the activation of FGF/FGFR2 signaling promotes osteoblastic differentiation caused by BMP-2 treatment in mesenchymal stem cells. Both BMPs and FGFs are key instructive signals produced at signaling centers of the limb bud (43, 44). The pattern of temporal and spatial expression of FGFs and BMPs strongly suggests cooperative actions of these signaling molecules during limb development (45). It has been reported that BMPs are expressed at the bone fracture site and that local application of rhFGF-2 at the fracture site accelerates fracture healing (46, 47). Additionally, the synergistic effect of FGF-4 in BMP-2-induced ectopic bone formation has also been observed (48). In our experiment, growth factors belonging to FGF family in the culture medium bind their receptors (FGFR2) and lead to the activation of FGF/FGFR2 signal pathway, coordinating with BMP-2 to induce osteogenesis. Overexpression of full-length FGFR2 or dominant negative form may enhance or inhibit the process, respectively.

However, in our study, we failed to the identify BMP2-responsive element in a long range of genomic DNA containing the proximal promoter region. We think that it may be located in a site beyond the proximal promoter, even downstream of the gene, acting as an enhancer. Although NF-Y only determines the basal expression of FGFR2 gene, it provides a regulatory base for BMP-2 to stimulate FGFR2 expression. We believe that NF-Y must play a physiologically important role in the regulation of BMP-2-induced FGFR2 expression and even osteogenesis, considering that FGFR2 is a positive regulator of ossification.

Taken together, our results lead to the hypothesis that NF-Y, characterized by histone-like protein structures, binds to the nucleosome bearing the CCAAT box and acts as a docking partner for recruiting acetyltransferase such as p300 and P/CAF (p300/CBP-associated factor) to the promoter. Then histones are hyperacetylated, and tight and compacted chromatin structure is disrupted with more accessibility. In summary, NF-Y might opens and maintains an accessible chromatin for basal activation of FGFR2 transcription.

REFERENCES

1. Nakamura, T., Hanada, K., Tamura, M., Shibanushi, T., Nigi, H., Tagawa, M., Fukumoto, S., and Matsumoto, T. (1995) *Endocrinology* **136,** 1276–1284
2. Noda, M., and Vogel, R. (1989) *J. Cell Biol.* **109,** 2529–2535
3. Reardon, W., Winter, R. M., Rutland, P., Pulleyn, L. J., Jones, B. M., and Malcolm, S. (1994) *Nat. Genet.* **8,** 98–103
4. Tavormina, P. L., Shiang, R., Thompson, L. M., Zhu, Y. Z., Wilkin, D. J., Lachman, R. S., Wilcox, W. R., Rimoin, D. L., Cohn, D. H., and Wasmuth, J. J. (1995) *Nat. Genet.* **9,** 321–328
5. Eswarakumar, V. P., Monsonego-Ornan, E., Pines, M., Antonopoulou, I., Morriss-Kay, G. M., and Lonai, P. (2002) *Development* **129,** 3783–3793
6. Mansukhani, A., Bellosta, P., Sahni, M., and Basilico, C. (2000) *J. Cell Biol.* **149,** 1297–1308
7. Evers, R., Kool, M., van Deemter, L., Janssen, H., Calafat, J., Oomen, L. C., Paulusma, C. C., Oude Elferink, R. P., Baas, F., Schinkel, A. H., and Borst, P. (1998) *J. Clin. Investig.* **101,** 1310–1319
8. Lemonnier, J., Delannoy, P., Hott, M., Lomri, A., Modrowski, D., and Marie, P. J. (2000) *Exp. Cell Res.* **256,** 158–167
9. Lemonnier, J., Hay, E., Delannoy, P., Lomri, A., Modrowski, D., Caverzasio, J., and Marie, P. J. (2001) *J. Bone Miner Res.* **16,** 832–845
10. Mantovani, R. (1998) *Nucleic Acids Res.* **26,** 1135–1143
11. Baxevanis, A. D., Arents, G., Moudrianakis, E. N., and Landsman, D. (1995) *Nucleic Acids Res.* **23,** 2685–2691
12. Motta, M. C., Caretti, G., Badaracco, G. F., and Mantovani, R. (1999) *J. Biol. Chem.* **274,** 1326–1333
13. Framson, P., and Bornstein, P. (1993) *J. Biol. Chem.* **268,** 4989–4996
14. Zwicker, J., Gross, C., Lucibello, F. C., Truss, M., Ehlert, F., Engeland, K., and Muller, R. (1995) *Nucleic Acids Res.* **23,** 3822–3830
15. Bellorini, M., Lee, D. K., Dantonel, J. C., Zemzoumi, K., Roeder, R. G., Tora, L., and Mantovani, R. (1997) *Nucleic Acids Res.* **25,** 2174–2181
16. Coustry, F., Sinha, S., Maity, S. N., and Crombrugghe, B. (1998) *Biochem. J.* **331,** 291–297
17. Frontini, M., Imbriano, C., diSilvio, A., Bell, B., Bogni, A., Romier, C., Moras, D., Tora, L., Davidson, I., and Mantovani, R. (2002) *J. Biol. Chem.* **277,** 5841–5848
18. Currie, R. A. (1998) *J. Biol. Chem.* **273,** 1430–1434
19. Miki, T., Fleming, T. P., Bottaro, D. P., Rubin, J. S., Ron, D., and Aaronson, S. A. (1991) *Science* **251,** 72–75
20. Raz, V., Kelman, Z., Avivi, A., Neufeld, G., Givol, D., and Yarden, Y. (1991) *Oncogene* **6,** 753–760
21. Rao, S., Procko, E., and Shannon, M. F. (2001) *J. Immunol.* **167,** 4494–4503
22. Su, L., Creusot, R. J., Gallo, E. M., Chan, S. M., Utz, P. J., Fathman, C. G., and Ermann, J. (2004) *J. Immunol.* **173,** 4994–5001
23. Lucas, M., Zhang, X., Prasanna, V., and Mosser, D. M. (2005) *J. Immunol.* **175,** 469–477
24. Thomas, R. M., Gao, L., and Wells, A. D. (2005) *J. Immunol.* **174,** 4639–4646
25. Yan, C., Wang, H., Toh, Y., and Boyd, D. D. (2003) *J. Biol. Chem.* **278,** 2309–2316
26. Francis, J., Babu, D. A., Deering, T. G., Chakrabarti, S. K., Garmey, J. C., Evans-Molina, C., Taylor, D. G., and Mirmira, R. G. (2006) *Mol. Endocrinol.* **20,** 3133–3145
27. Brettingham-Moore, K. H., Rao, S., Juelich, T., Shannon, M. F., and Holloway, A. F. (2005) *Nucleic Acids Res.* **33,** 225–234
28. Narlikar, G. J., Fan, H. Y., and Kingston, R. E. (2002) *Cell* **108,** 475–487
29. Landsberger, N., and Wolffe, A. P. (1995) *Mol. Cell. Biol.* **15,** 6013–6024
30. Anderson, J. D., Lowary, P. T., and Widom, J. (2001) *J. Mol. Biol.* **307,** 977–985
31. Gui, C. Y., and Dean, A. (2001) *Mol. Cell. Biol.* **21,** 1155–1163
32. Duan, Z., Stamatoyannopoulos, G., and Li, Q. (2001) *Mol. Cell. Biol.* **21,** 3083–3095
33. Dennig, J., Hagen, G., Beato, M., and Suske, G. (1995) *J. Biol. Chem.* **270,** 12737–12744
34. Kollmar, R., Sukow, K. A., Sponagle, S. K., and Farnham, P. J. (1994) *J. Biol. Chem.* **269,** 2252–2257

35. Blake, M. C., Jambou, R. C., Swick, A. G., Kahn, J. W., and Azizkhan, J. C. (1990) *Mol. Cell. Biol.* **10,** 6632–6641
36. Avivi, A., Skorecki, K., Yayon, A., and Givol, D. (1992) *Oncogene* **7,** 1957–1962
37. Chiang, C. M., and Roeder, R. G. (1995) *Science* **267,** 531–536
38. Sinha, S., Kim, I. S., Sohn, K. Y., de Crombrugghe, B., and Maity, S. N. (1996) *Mol. Cell. Biol.* **16,** 328–337
39. Arents, G., Burlingame, R. W., Wang, B. C., Love, W. E., and Moudrianakis, E. N. (1991) *Proc. Natl. Acad. Sci. U. S. A.* **88,** 10148–10152
40. Caretti, G., Motta, M. C., and Mantovani, R. (1999) *Mol. Cell. Biol.* **19,** 8591–8603
41. Gorzowski, J. J., Eckerley, C. A., Halgren, R. G., Mangurten, A. B., and Phillips, B. (1995) *J. Biol. Chem.* **270,** 26940–26949
42. Caretti, G., Salsi, V., Vecchi, C., Imbriano, C., and Mantovani, R. (2003) *J. Biol. Chem.* **278,** 30435–30440
43. Martin, G. R. (1998) *Genes Dev.* **12,** 1571–1586
44. Xu, X., Weinstein, M., Li, C., and Deng, C. (1999) *Cell Tissue Res.* **296,** 33–43
45. Merino, R., Ganan, Y., Macias, D., Economides, A. N., Sampath, K. T., and Hurle, J. M. (1998) *Dev. Biol.* **200,** 35–45
46. Nakamura, T., Hara, Y., Tagawa, M., Tamura, M., Yuge, T., Fukuda, H., and Nigi, H. (1998) *J. Bone Miner Res.* **13,** 942–949
47. Radomsky, M. L., Thompson, A. Y., Spiro, R. C., and Poser, J. W. (1998) *Clin. Orthop. Relat. Res.* **355,** (suppl.) 283–293
48. Kubota, K. I. S., Kuroda, S., Oida, S., Iimura, T., Duarte, W. R., Ohya, K., Ishikawa, I., and Kasugai, S. (2002) *Bone* (*NY*) **31,** 465–471